Influence of Sodium and Rubidium Postdeposition Treatment on the Quasi-Fermi Level Splitting of $Cu(In,Ga)Se_2$ Thin Films

Max Hilaire Wolter, Benjamin Bissig, Enrico Avancini, Romain Carron, Stephan Buecheler, Philip Jackson, and Susanne Siebentritt

***Abstract*—The influence of sodium and rubidium postdeposition treatment on the quality of $Cu(In,Ga)Se_2$ thin-film absorbers is investigated. The quasi-Fermi level splitting (QFLS), measured via photoluminescence (PL), is used as the metric of quality of the absorber. To evaluate the QFLS values in the graded absorber of state-of-the-art devices, it is necessary to know at which location the luminescence is generated. Here we show, by measuring the PL in different geometries, that the photons originate from the global band gap minimum inside the bulk. We use this knowledge to compare the QFLS in different absorbers, where our results show that the QFLS is higher in absorbers that were treated with NaF + RbF than in absorbers that were only treated with NaF or not treated at all. We attribute this increase to a reduced nonradiative recombination, even before cadmium sulfide deposition. A decreased difference between QFLS and open-circuit voltage in the corresponding finished solar cells also reveals an improved CdS/CIGS interface. Both effects ultimately lead to a higher efficiency.**

I. Introduction

THE beneficial effects of alkali elements, especially sodium, on the performance of chalcopyrite solar cells based on $Cu(In,Ga)Se_2$ (CIGS) absorbers were discovered more than 20 years ago [1]. It was found that Na naturally diffuses from the alkali containing soda lime glass (SLG) substrate into the absorber during the high-temperature growth process. In solar cells grown on alkali-free substrates, such as the flexible polyimide films, the alkali elements would need to be added extrinsically in order to benefit from their influence. As a direct consequence, the NaF postdeposition treatment (PDT), where sodium is added in an additional step after film growth, was introduced [2]. Nowadays, all alkalis have been used in a PDT. For example, the absorber of a solar cell grown on a flexible substrate and reaching 20.4% record efficiency was treated with both sodium and potassium [3]. PDT with even heavier alkalis, such as rubidium, paved the way for the improvement of the efficiencies of CIGS solar cells up to 22.6% [4] and most recently to record efficiencies of 22.9% [5].

While the different alkali PDTs are clearly beneficial for the performance of the CIGS solar cells, the underlying reasons for the improvement have not yet been fully understood. To date, most research was conducted on the sodium and potassium PDTs, which had been developed first. In this context, the postdeposition processes involving KF have been shown to cause a Cu- and Ga-depleted surface region [3], [6]. The surface region is thought to facilitate the in-diffusion of cadmium and consequently the formation of Cd_{Cu} donor levels during the deposition of CdS [3], [7], [8]. Furthermore, the NaF + KF PDT also induces a band gap widening at the absorber surface [6], [9]. Both effects can lead to a reduction of CdS/CIGS interface recombination and consequently a higher open-circuit voltage V_{OC} and fill factor of the solar cell.

Not only the interface is changed, but also the bulk absorber is influenced by the PDT. A recent study has found that the addition of KF, and a combined NaF + KF PDTs influence the doping concentration as compared with untreated, alkali-free absorbers [7]. Another study reveals that this change in the doping level directly leads to a longer carrier lifetime and a higher photoluminescence signal. Both these effects are a direct consequence of the reduction of nonradiative recombination [10].

Thus, so far, numerous studies have revealed that the PDTs involving both sodium and potassium improve the solar cell device by influencing both the interface and the bulk absorber. However, the influence of the heavier alkalis, such as rubidium and cesium, is currently less investigated.

We measure intensity calibrated photoluminescence (PL) on absorbers having undergone different PDTs. The PL is measured on both bare absorbers and covered absorbers by a cadmium sulfide layer. By determining the quasi-Fermi level splitting (QFLS), which is an upper limit for the V_{OC} [11], [12],

Manuscript received May 31, 2018; revised June 27, 2018; accepted July 7, 2018. Date of publication July 23, 2018; date of current version August 20, 2018. This work was supported in part by the European Union's Horizon 2020 research and innovation program under Grant 641004 (Sharc25) and in part by the Swiss State Secretariat for Education, Research and Innovation (SERI) under Contract number 15.0158. *(Corresponding author: Max Hilaire Wolter.)*

M. H. Wolter and S. Siebentritt are with the Physics and Materials Science Research Unit, Laboratory for Photovoltaics, University of Luxembourg, Belvaux 4422, Luxembourg (e-mail: max.wolter@uni.lu; susanne.siebentritt@uni.lu).

B. Bissig, E. Avancini, R. Carron, and S. Buecheler are with the Laboratory for Thin Films and Photovoltaics, Empa – Swiss Federal Laboratories for Materials Science and Technology, Dübendorf 8600, Switzerland (e-mail: benjamin.bissig@empa.ch; enrico.avancini@empa.ch; Romain.carron@empa.ch; stephan.buecheler@empa.ch).

P. Jackson is with the Zentrum für Sonnenenergie- und Wasserstoff-Forschung Baden-Württemberg, Stuttgart 70565, Germany (e-mail: philip.jackson@zsw-bw.de).

This paper has supplementary downloadable material available at http://ieeexplore.ieee.org.

Color versions of one or more of the figures in this paper are available online at http://ieeexplore.ieee.org.

Digital Object Identifier 10.1109/JPHOTOV.2018.2855113

and comparing its value between the samples, it is possible to investigate the direct influence of the alkali elements either on the absorber alone or including the CdS/CIGS interface.

The QFLS is evaluated on the high-energy slope of the measured PL spectra. For the samples measured in this study, two issues need to be resolved first before determining the QFLS and comparing its value between the samples. The first issue is the occurrence of interference effects in state-of-the-art CIGS thin films that are mainly due to the presence of a graded band gap and a smooth surface [13]. In a previous study [14], we have shown that these interference effects do not affect the high-energy slope of the PL spectra and can thus be ignored for the determination of the QFLS. The second issue is the graded band gap and the question at which point in the graded absorber the emitted photoluminescence originates.

The graded band gap was first introduced back in the 1994 when a novel three-stage process was presented by Gabor *et al.* [15]. This absorber growth process consisted of the formation of a double-graded Ga profile across the film thickness with an elevated Ga concentration (i.e., higher band gap) present at both the surface and at the back of the absorber and a notch of low Ga concentration and band gap in between. One primary consequence of this graded band gap was a reduced recombination rate in the absorber and hence an improved open-circuit voltage [16]. Since then, the double-graded band gap has been extensively investigated (see e.g., [17]) and is responsible for the achievement of several milestones in the history of CIGS, such as the first 18.7% record efficiency on flexible polymer films in 2011 [18]. In the most recent state-of-the-art CIGS absorber, the Ga profile is further characterized by an additional Ga minimum at the surface (see e.g., [19, Fig. 2]). The intricate nature of the graded band gap affects the incoming light absorption, the subsequent carrier transport, and finally the recombination. These properties are all integral to the process of photoluminescence. Thus, the influence of the graded band gap on the emitted PL needs to be understood.

The paper is split into two parts. The first part investigates the origin of the emitted PL along the graded band gap. This is done by generating charge carriers both at the front and at the back of the absorber and by investigating their emission spectra. The second part of the paper deals with the determination of the QFLS splitting and the influence of the alkali PDTs on the CIGS thin films.

II. Experimental Details

A. Growth Process

The measurements that will be shown in Section III of the paper are done on a cadmium sulfide (CdS)-covered CIGS absorber grown in a high-temperature multistage coevaporation process on molybdenum-coated SLG. Details about this growth process can be found in [4]. In this particular case, the surface exhibits a significant roughness, leading to an interference-free PL spectrum at room temperature.

The CIGS absorbers measured in Section IV of the paper are grown in a low-substrate temperature multistage coevaporation process on a $5 \times 5\,\mathrm{cm}^2$ molybdenum-coated SLG. In order to avoid any in-diffusion of alkali elements from the SLG and to mimic the process on polyimide foil, an SiO_2 barrier layer is deposited between the molybdenum back contact and the substrate. After the growth process, the CIGS absorbers receive different PDTs. As a measure of reference, sample A does not receive any PDT. Sample B receives an NaF only PDT, while sample C receives a combined NaF + RbF PDT. For each sample, half of the $5 \times 5\,\mathrm{cm}^2$ absorber is used for solar cell processing, one-eighth is kept as bare absorber, and another one-eighth is covered by a CdS buffer layer that is deposited by chemical bath deposition (CBD) to protect the absorber surface from degradation [20]. Both bare and CdS-covered absorbers, $1.25 \times 2.5\,\mathrm{cm}^2$ in size, are used for optical characterization. Details about the growth process, PDT, and CBD can be found in [3], [7], and [18]. The detailed elemental composition of the samples is determined by X-ray fluorescence (XRF) measurements. Secondary ion mass spectrometry (SIMS) measurements are used to evaluate the gallium gradient and subsequently calculate the band gap minimum. The Ga profile in each case is very similar to one of the samples grown by high-temperature coevaporation that is used in Section III. Scanning electron microscopy (SEM) cross sections are measured to determine the thickness of the samples. The results of these measurements, along with selected current density–voltage parameters are listed in Table I.

B. Optical Characterization

In the intensity calibrated photoluminescence experiments, the samples are excited by the 660 nm line of a diode laser. The photon flux is set to $2.76 \cdot 10^{17}$ photons $\mathrm{cm}^{-2}\ \mathrm{s}^{-1}$, which is equivalent to the flux of an AM1.5 sun spectrum above 1.1 eV. The laser spot used for the PL measurements has a diameter of 2.6 mm as measured by a CMOS camera. Two off-axis parabolic UV-enhanced aluminum mirrors collect and redirect the emitted photoluminescence into a spectrometer with 303 mm focal length, where it is dispersed and detected by a 512 element InGaAs array. The measurements are performed at room temperature and are spectrally corrected by using a commercial calibrated halogen lamp.

The photoluminescence experiments that investigate the graded band gap, presented in Section III, are not based on intensity calibration but are measured by exciting the samples with a constant photon flux of approx. $6.26 \cdot 10^{16}$ photons $\mathrm{cm}^{-2}\ \mathrm{s}^{-1}$. The rest of the optics is as described above.

III. Origin of Photoluminescence

Photoluminescence is the radiative recombination of photogenerated charge carriers. The process is initiated by illuminating a semiconductor, typically with the monochromatic light of a laser. If the energy of the incoming light is higher than the band gap, the photons are absorbed and create electron–hole pairs inside the semiconducting absorber. After excitation and at room temperature, the charge carriers thermally relax with the lattice and diffuse along the graded band gap structure into a minimum energy state before they then undergo a radiative recombination process that results in the emission of photons from the

TABLE I
SUMMARY OF SAMPLE PROPERTIES

Sample	PDT	GGI	Band gap minimum (eV)	Thickness (μm)	Voc (mV)	η (%)
A	None	0.34	1.132	2	581	13.3
B	NaF	0.35	1.138	1.85	685	16.5
C	NaF + RbF	0.37	1.137	1.9	708	18.2

Indicated are the values of selected parameters that were measured with XRF, SIMS, and SEM. The indicated Ga/(Ga + In) (GGI) ratio is averaged over the whole absorber. The differences in the average GGI between the samples originate from the different Ga contents toward the back of the absorber. The band gap minimum in eV was calculated according to $1.004\ (1–x) + 1.663\ x – 0.033\ x\ (1–x)$, where x is the GGI ratio at the notch [24]. The thickness relates to the absorber only. The parameter η represents the total area efficiency measured without anti-reflection coating. Both V_{OC} and η values represent averages over six side-by-side cells.

sample. These emitted photons are captured and measured as photoluminescence. The PL spectrum of such a recombination process shows a broad peak centered around the energy of the transition.

While the underlying principle of photoluminescence is relatively straightforward, its real behavior can be influenced in numerous instances during the different stages. For example, a crucial aspect is the absorption of the incoming photon flux that depends on the absorption coefficient of the absorber. The latter quantity thus heavily influences the penetration depth of the incident light and the subsequent charge carrier generation profile inside the absorber. Given the graded structure of the band gap and the diffusion properties of the excited charge carriers, the emitted photoluminescence can originate from the two band gap minima: One located at the surface and one located inside the bulk. A typical representation of both these band gap minima is visualized in the inset of Fig. 2. To evaluate the meaning of the extracted QFLS, the knowledge of the exact PL origin from the absorber is crucial.

The origin of the photoluminescence signal can be investigated by illuminating the absorber either from the surface, where the charge carriers could diffuse into the surface band gap minimum, or from the back, where the charge carriers are expected to diffuse into the lower band gap minimum inside the bulk. Since it is not possible to illuminate the absorbers from the back due to the presence of the blocking molybdenum back contact, the absorbers first have to be exfoliated from the Mo-coated glass substrate. The whole experimental process is schematically summarized in Fig. 1. In a first step [see Fig. 1(a)], the PL is measured in the standard or normal (N) configuration on a sample stack that consists of a CdS-covered CIGS absorber grown on a Mo-coated SLG substrate. In a second step [see Fig. 1(b)], the exfoliation process is prepared by taking an additional SLG substrate and gluing it to the CIGS surface (a transparent epoxy glue is used). In order to investigate the influence of the SLG and glue on the PL signal, the PL is measured through the glass and the glue from the front of the film (G). In a third and final step [see Fig. 1(c)], the absorber is exfoliated from its original substrate and the PL is measured from the front through the glass (ExG) and from the back that now lies bare (ExB).

The four different PL spectra are shown in Fig. 2 in a semilogarithmic representation to facilitate their comparison. The red curve shows the PL spectrum in normal configuration (N) and acts as a reference spectrum. The blue curve shows that, after gluing an SLG on top of the sample (G), the PL intensity decreases. This decrease is partly due to a reduced excitation density from the laser light since a fraction of the light is scattered by the SLG and glue before reaching the sample, and partly due to the emitted PL light also being scattered by the glue and SLG before reaching the detector. Besides the difference in PL intensity, both PL spectra measured in configuration (N) and (G) are identical. This means that the peaks share the same emission origin and that a reduced excitation does not lead to a shift of the transition peak. After the exfoliation process, the PL spectrum measured from the back (ExB) shows two peaks (yellow curve). We attribute the high-energy peak to a transition at the back and discuss it briefly further below. Additionally, we attribute the low-energy peak in the (ExB) configuration to the recombination from the band gap minimum inside the bulk as the PL can only be emitted from the bulk minimum band gap if excited entirely from the back. Comparing the low-energy peak of the (ExB) configuration to the peak of the reference (N) configuration, we notice an energy difference of 14 meV between both peaks. This energy difference could indicate that the PL is emitted from a different band gap minimum in the (ExB) configuration than in the (N) configuration. However, if we compare the PL spectra measured in the (G) and (ExG) configuration (green curve), we notice the same energy shift between the peaks. Since we have the same excitation profile in the (G) and (ExG) configuration, the PL has to be emitted from the same band gap minimum. Finally, comparing the PL spectra of the (ExG) and (ExB) configuration, the low-energy peak positions are identical, indicating that the PL is emitted from the same band gap minimum inside the bulk in all four configurations. This means there must be a different explanation for the observed energy shift of the peaks of the exfoliated absorbers.

Additional experiments and investigations involving different exfoliation processes (see Supplementary material) indicate that the redshift that sets in after the exfoliation process could be due to a relaxation of the crystalline structure of the CIGS absorber. Standard CIGS absorbers that are grown on Mo-coated SLG are likely to be strained due to the lattice mismatch between CIGS and Mo. The exfoliation process removes the CIGS from the Mo and thus the CIGS crystal is able to relax resulting in a structure with lower band gap. Thus, the redshift is just a slightly reduced band gap of the CIGS absorber as a consequence of the exfoliation process. During the measurements shown here, we waited 6 h between gluing the glass onto the CIGS surface and the actual exfoliation process. In other experiments, as shown in the Supplementary materials, we waited 96 and 168 h before

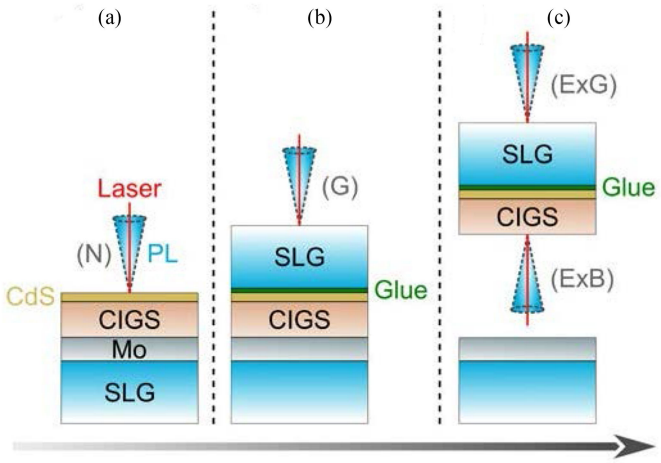

Fig. 1. Schematic visualization of the exfoliation process and accompanying PL measurements. (a) Normal (N) PL measurement done by illuminating the absorber from the front with a laser (red) and measuring the resulting PL (light-blue cone) on a sample stack consisting of a soda-lime glass (SLG) substrate, a molybdenum (Mo) back contact and a CIGS absorber covered by a CdS layer. (b) Preparation of the exfoliation process: An additional SLG is glued on top of the absorber. Process monitoring by measuring PL through the glass and glue (G). (c) PL measurements after exfoliation from the front through the glass (ExG) and from the back (ExB).

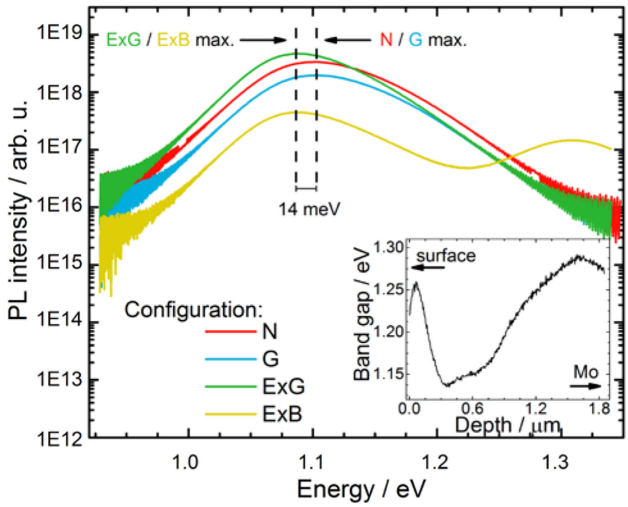

Fig. 2. PL spectra measured at the different stages of the exfoliation process. The red curve shows the PL measured in the normal (N) configuration. The blue curve shows the PL measured through the glass after the glass was glued to the absorber surface (G). The green curve shows the PL measured through the glass after the absorber is exfoliated from its original Mo-coated substrate (ExG). The yellow curve shows the PL measured from the back of the exfoliated absorber (ExB). The main peak of both (ExG) and (ExB) PL spectra shows a redshift of 14 meV compared with the PL peak of the (N) and (G) configurations. The PL spectrum in the (ExB) configuration shows an additional peak at higher energies, indicating an additional recombination activity at the back of the absorber. The inset shows the band gap profile versus absorber depth grown at low temperature and as measured by SIMS and XRF and serves as an example to visualize the band gap minima located at the surface and inside the bulk.

exfoliation and saw a considerable reduction of the redshift compared with when the exfoliation process is done just hours after the gluing in both these cases. These findings indicate that the shorter the "curation" time of the glue, i.e., the softer the glue is at the time of exfoliation, the stronger the strain release after exfoliation and thus the stronger the redshift. The more time the glue has to harden, the weaker the strain release after exfoliation and thus the smaller the band gap change. Finally, we need to mention that it is difficult to theoretically predict the band gap shift caused by the strain because of the complex alloy structure of polycrystalline CIGS with a graded Ga content. We propose the abovementioned changes to the crystalline CIGS structure as an explanation for the redshift based only on PL measurements.

The reduction in band gap also explains the higher PL intensity measured in the (ExG) configuration as compared with the (G) configuration. Looking at the high-energy slope of the PL spectra in both these configurations, we can see that their QFLS are identical. The same QFLS in a lower band gap means higher carrier concentration and thus a higher radiative efficiency.

Lastly, the PL spectrum measured in the (ExB) configuration shows a significant drop in PL intensity as well as the presence of an additional, high-energy peak. The energy of this latter peak is approximately 1.31 eV and is likely due to the recombination of excited charge carriers at the back of the absorbers, where the gallium content and the band gap are highest. Generally, the three-stage process leads to smaller grains at the back contact (see e.g., [21] or [22]). It can be expected that the presence of a higher density of grain boundaries leads to stronger nonradiative recombination near the rear of the film, which explains why the overall PL intensity in the (ExB) configuration with illumination through the rear of the film is low compared with the other configurations. Additionally, for the 1.31 eV peak to appear in the PL spectrum, the generated charge carriers also have to radiatively recombine near the rear of the absorber. A possible explanation is that the grain boundaries also represent a transport barrier and only a reduced fraction of charge carriers generated further inside the bulk is able to diffuse to the minimum band gap and recombine from there, further explaining the reduced PL intensity of the main peak in the (ExB) configuration.

In addition, we also conducted PL measurements with different wavelength excitation (514.5, 660, 980 nm) in normal configuration resulting in different penetration depths of the laser light (not shown here). The resulting PL spectra revealed no energy shift of the peak, underlining our findings that the luminescence originates from the band gap notch inside the absorber film. Furthermore, Bauer *et al.* conducted etching and subsequent PL experiments on absorbers, whose band gap showed a minimum inside the bulk but no surface band gap minimum and came to a similar conclusion [23]. To summarize, the exfoliation experiments have shown that the PL is originating from the band gap minimum inside the bulk of the CIGS absorbers.

IV. Influence of Sodium and Rubidium Postdeposition Treatment

The findings of Section III reveal that the photoluminescence in graded band gap absorbers originates from the band gap minimum. In order to compare quantities that depend on the band gap, such as the QFLS or open-circuit voltage (V_{OC}) between different absorbers or solar cells, it is crucial to know the exact

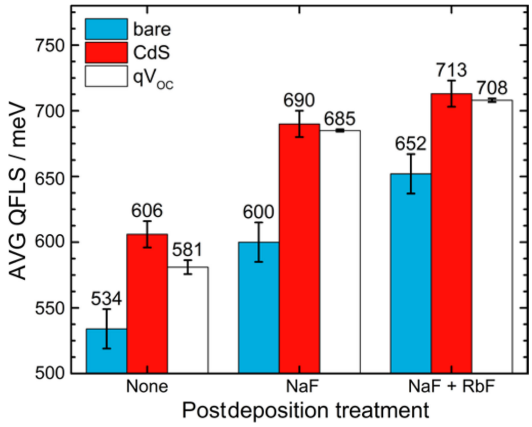

Fig. 3. Bar plot of the average QFLS for bare (blue) and CdS-covered (red) CIGS absorbers having undergone different postdeposition treatments. For comparison, the qV_{OC} (white) of the finished solar cells are also shown. Also included are error bars. We attribute an error bar of 10 meV to the QFLS of CdS-covered absorber that takes into account the standard deviations of the different measurement spots as well as the imprecision of the fits. We attribute a slightly higher error bar of 15 meV to the QFLS of the bare absorbers since their reduced signal and consequently larger signal-to-noise ratio lead to a larger fit imprecision. Finally, the error bars attributed to the qV_{OC} of the solar cells represent the standard deviation of their values measured on six side-by-side cells.

value of the band gap minimum. As mentioned in Section II, the samples underwent XRF and SIMS measurements to determine the exact gallium content throughout the absorber. From the gallium concentration, the band gap minimum inside the bulk was calculated (as described in the caption of Table I). It was found that the samples at hand share an almost identical band gap minimum.

With this knowledge, the influence of different alkali PDTs on CIGS absorbers can be investigated. The method to extract the QFLS from the photoluminescence spectra is adapted from [25]. In the fitting routine, the temperature was held constant at 296 K, which was the ambient temperature of the laboratory during the experiment, since incomplete absorption can lead to an overestimation of the temperature, if determined from a fit to the high-energy slope of the PL spectrum, and thus to an underestimation of the QFLS [26]. In order to account for any inhomogeneities in the samples, the QFLS was determined and averaged from PL spectra taken at three different spots on each sample. A quick statistical analysis shows that, at worst, the QFLS of the CdS-covered absorber lie all within 4 meV of the average value. For the bare absorbers, the largest standard deviation amounts to 4.5 meV. Since these standard deviations are small (below 0.8%), the samples can be considered as being very homogeneous on a macroscopic scale. The average QFLS are summarized in Fig. 3.

First, we discuss only the QFLS that was extracted from the CdS-covered absorbers (red bars in Fig. 3). The data show that the QFLS increases with NaF treatment and again with NaF + RbF treatment. The higher the QFLS with constant band gap and at constant illumination, the lower the nonradiative recombination rate and thus the higher the density of photogenerated charge carriers. Since the QFLS is directly proportional to the logarithm of the PL intensity, an increase in the QFLS is always related to an increase in the radiative recombination. Thus, what is reduced is the nonradiative recombination. Since the band gap minima of the different samples are equal within 6 meV (see Table I), we can conclude that the alkali treatment reduces nonradiative recombination and that this reduction is stronger for samples treated with heavier alkalis.

Next, comparing the QFLS values of the CdS-covered absorbers to the V_{OC} of the finished solar cells, we see that the QFLS follows the same trend as the V_{OC}. Thus, we conclude that the absorber improvement from the alkali PDT is independent of the band bending that is caused by the aluminum-doped ZnO during the fabrication of the solar cell device. Additionally, since the QFLS represents the maximal possible V_{OC} of the absorber, the difference between QFLS and qV_{OC} describes the loss in V_{OC} upon finishing the solar cell. This difference amounts to 25 meV in the case of the untreated sample and to 5 meV in both NaF only and NaF + RbF treated samples. The smaller loss in V_{OC} for both treated samples compared with the untreated sample could be attributed to a reduced recombination near the CdS/CIGS interface in the finished device.

Finally, we look at the QFLS of the bare absorbers visualized by the blue bars in Fig. 3. The QFLS is considerably lower in the bare absorbers than in the absorbers with CdS. This is due to their exposure to air which leads to a swift degradation of their surface resulting in an enhanced nonradiative recombination and smaller QFLS [20]. Nonetheless, the QFLS of the bare absorbers follows the same trend as for the absorbers with CdS, i.e., it increases with heavier alkali PDT. This indicates that already the absorber (and its surface) is improved, even without the interface with CdS. Since the QFLS of bare absorbers critically depends on their degradation in air, one could argue that the alkali treatment simply reduces the degradation effect by passivating the surface with an additional layer [27]. However, the NaF treatment does not lead to a distinct surface layer. Furthermore, the bare absorbers were all several weeks in air, allowing thus ample diffusion of atmosphere components through any surface layer. Additionally, in another sample series with treatments with various alkalis (K, Rb, Cs—not shown here), we see similar improvements of the QFLS of bare absorbers that follow the trend of the V_{OC} improvements with those treatments. Therefore, we attribute the higher QFLS in bare absorbers after alkali treatment to a reduction of the nonradiative recombination in the absorber, even without the CdS interface.

Combining the argumentations from the above observations, we can say that the PDT with heavier alkalis directly improves the absorber itself by reducing the nonradiative recombination rate. Additionally, a comparison between the QFLS of the CIGS/CdS absorber and the V_{OC} of the finished device reveals reduced electronic losses at the CdS/CIGS interface for both samples treated with NaF only and a combined NaF + RbF PDT compared with the sample without treatment. Furthermore, our results reveal no reduction of electronic losses at the interface between both alkali treatments. Ultimately, both the reduction of nonradiative recombination and improved CdS/CIGS interference effects lead to a larger V_{OC} and a higher efficiency.

V. Conclusion

State-of-the-art thin-film CIGS absorbers exhibit a local band gap minimum at the surface and a global band gap minimum inside the bulk as a consequence of a doubly graded gallium profile. While this graded band gap structure is beneficial for the solar cell, its influence on measurements methods, such as photoluminescence, is not obvious. The band gap structure could, *a priori*, suggest that radiative recombination is occurring from either the surface or bulk band gap or from a combination of both. For the correct interpretation of photoluminescence measurements, it is crucial to understand the origin of the emitted PL. Experiments on standard and exfoliated absorbers in different configurations have revealed that the PL originates from the global band gap minimum inside the bulk and not from the surface. We made use of that knowledge and investigated the influence of different PDTs on the CIGS absorbers. Intensity calibrated photoluminescence measurements on bare and CdS-covered untreated, NaF treated, and NaF + RbF treated absorbers were conducted in order to determine and compare the QFLS. Our results reveal an increased QFLS in both bare and CdS-covered absorbers that were treated with heavier alkalis. We attribute this increase to a reduced nonradiative recombination in the absorber. This effect is stronger with heavier alkalis. Additionally, our results also reveal a reduction of the electronic losses at the CdS/CIGS interface. Both effects ultimately lead to a higher solar cell efficiency.

References

[1] J. Hedstrom *et al.*, "ZnO/CdS/Cu(In,Ga)Se2 thin film solar cells with improved performance," in *Proc. Conf. Rec. 23rd IEEE Photovolt. Spec. Conf.*, 1993, pp. 364–371.

[2] D. Rudmann, D. Bremaud, H. Zogg, and A. N. Tiwari, "Na incorporation into $Cu(In,Ga)Se_2$ for high-efficiency flexible solar cells on polymer foils," *J. Appl. Phys.*, vol. 97, no. 8, 2005, Art. no. 084903.

[3] A. Chirilă *et al.*, "Potassium-induced surface modification of $Cu(In,Ga)Se_2$ thin films for high-efficiency solar cells," *Nature Mater.*, vol. 12, pp. 1107–1111, 2013.

[4] P. Jackson *et al.*, "Effects of heavy alkali elements in $Cu(In,Ga)Se_2$ solar cells with efficiencies up to 22.6%," *Phys. Status Solidi RRL*, vol. 10, no. 8, pp. 583–586, 2016.

[5] Solar Frontier Press release. 2017. [Online]. Available: http://www.solar-frontier.com/eng/news/2017/1220_press.html. Accessed on: Jan. 2018.

[6] P. Pistor *et al.*, "Experimental indication for band gap widening of chalcopyrite solar cell absorbers after potassium fluoride treatment," *Appl. Phys. Lett.*, vol. 105, 2014, Art. no. 063901.

[7] F. Pianezzi *et al.*, "Unveiling the effects of post-deposition treatment with different alkaline elements on the electronic properties of CIGS thin film solar cells," *Phys. Chem. Chem. Phys.*, vol. 16, pp. 8843–8851, 2014.

[8] B. Ümsur *et al.*, "Investigation of the potassium fluoride post deposition treatment on the CIGSe/CdS interface using hard X-ray photoemission spectroscopy – a comparative study," *Phys. Chem. Chem. Phys.*, vol. 18, pp. 14129–14138, 2016.

[9] E. Handick *et al.*, "Potassium postdeposition treatment-induced band gap widening at $Cu(In,Ga)Se_2$ surfaces – reason for performance leap?," *ACS Appl. Mater. Interfaces*, vol. 7, no. 49, pp. 27414–27420, 2015.

[10] I. Khatri, H. Fukai, H. Yamaguchi, M. Sugiyama, and T. Nakada, "Effect of potassium fluoride post-deposition treatment on $Cu(In,Ga)Se_2$ thin films and solar cells fabricated onto sodalime glass substrates," *Sol. Energy Mater. Sol Cells*, vol. 155, pp. 280–287, 2016.

[11] P. Würfel, *The Physics of Solar Cells*. Hoboken, NJ, USA: Wiley, 2009.

[12] T. Unold and L. Gütay, "Photoluminescence analysis of thin-film solar cells" in *Advanced Characterization Techniques for Thin Film Solar Cells*, D. Abou-Ras, T. Kirchartz, and U. Rau, Eds. Berlin, Germany: Wiley, 2001, p. 151.

[13] J. K. Larsen *et al.*, "Interference effects in photoluminescence spectra of Cu_2ZnSnS_4 and $Cu(In,Ga)Se_2$ thin films," *J. Appl. Phys.*, vol. 118, 2015, Art. no. 035307.

[14] M. H. Wolter *et al.*, "Correcting for interference effects in the photoluminescence of $Cu(In,Ga)Se_2$ thin films," *Phys. Status Solidi C*, vol. 14, 2017, Art. no. 1600189.

[15] A. M. Gabor *et al.*, "High-efficiency $CuIn_xGa_{1-x}Se_2$ solar cells made from $(In_x, Ga_{1-x})_2Se_3$ precursor films," *Appl. Phys. Lett.*, vol. 65, no. 2, pp. 198–200, 1994.

[16] M. A. Contreras *et al.*, "Graded band-gap $Cu(In,Ga)Se_2$ thin-film solar cell absorber with enhanced open-circuit voltage," *Appl. Phys. Lett.*, vol. 63, no. 13, pp. 1824–1826, 1993.

[17] W. Witte *et al.*, "Gallium gradients in Cu(In,Ga)Se2 thin-film solar cells," *Prog. Photovolt., Res. Appl.*, vol. 23, pp. 717–733, 2015.

[18] A. Chirilă *et al.*, "Highly efficient $Cu(In,Ga)Se_2$ solar cells grown on flexible polymer films," *Nature.Mater.*, vol. 10, pp. 857–861, 2011.

[19] P. Jackson *et al.*, "Properties of $Cu(In,Ga)Se_2$ solar cells with new record efficiencies up to 21.7%," *Phys. Status Solidi RRL*, vol. 9, pp. 28–31, 2015.

[20] D. Regesch *et al.*, "Degradation and passivation of CuInSe2," *Appl. Phys. Lett.*, vol. 101, no. 11, 2012, Art. no. 112108.

[21] M. Powalla *et al.*, "High-efficiency Cu(In,Ga)Se2 cells and modules," *Sol. Energy Mater. Sol. Cells*, vol. 119, pp. 51–58, 2015.

[22] K. Ramanathan *et al.*, "Properties of 19.2% efficiency ZnO/CdS/CuInGaSe2 thin-film solar cells," *Prog. Photovolt. Res. Appl.*, vol. 11, pp. 225–230, 2015.

[23] G. H. Bauer *et al.*, "Depth dependent optoelectronic properties of Cu(In,Ga)Se2 with lateral resolution in the micron/submicron scale from luminescence studies," *Energy Procedia*, vol. 10, pp. 208–212, 2011.

[24] R. Carron *et al.*, "Refractive indices of layers and optical simulations of Cu(In,Ga)Se2 solar cells," *Sci. Technol. Adv. Mater.*, vol. 19, no. 1, pp. 396–410, 2018.

[25] F. Babbe, L. Choubrac, and S. Siebentritt, "Quasi Fermi level splitting of Cu-rich and Cu-poor Cu(In,Ga)Se2 absorber layers," *Appl. Phys. Lett.*, vol. 109, 2016, Art. no. 082105.

[26] G. Rey *et al.*, "Absorption coefficient of semiconductor thin-films: measurement from photoluminescence," *Phys. Rev. Appl.*, vol. 92018, Art. no. 064008.

[27] P. Reinhard *et al.*, "Alkali-templated surface nanopatterning of chalcogenide thin films: A novel approach toward solar cells with enhanced efficiency," *Nano Lett.*, vol. 15, pp. 3334–3340, 2015.

Authors' photographs and biographies not available at the time of publication.